Role of the Extracellular Loops of the Thyrotropin-Releasing Hormone Receptor: Evidence for an Initial Interaction with Thyrotropin-Releasing Hormone†

Jeffrey H. Perlman,*,‡ Anny-Odile Colson,§ Rahul Jain,|| Bryan Czyzewski,‡ Louis A. Cohen,||,⊥ Roman Osman,§ and Marvin C. Gershengorn‡

Division of Molecular Medicine, Department of Medicine, Cornell University Medical College and The New York Hospital, NewYork, New York 10021, Department of Physiology and Biophysics, Mount Sinai School of Medicine of the City University of New York, New York, New York 10029, and Laboratory of Bioorganic Chemistry, National Institute of Diabetes and Digestive and Kidney Diseases, National Institutes of Health, Bethesda, Maryland 20892

Received June 4, 1997; Revised Manuscript Received September 29, 1997⊗

ABSTRACT: Thyrotropin-releasing hormone (TRH), like most small ligands, appears to bind within the seven transmembrane-spanning helices (TMs) of its G protein-coupled receptor (TRH-R). A role for the extracellular loops (ECLs) of TRH-R has not been established. We substituted residues in the ECLs of TRH-R and show that Tyr-181 is important for high-affinity binding because its substitution leads to a 3700-fold lowering of the estimated affinity compared to wild-type TRH-R. Using TRH analogues, we provide evidence that there is a specific interaction between Tyr-181 in ECL-2 and the pyroGlu moiety of TRH. It was previously suggested that the pyroGlu of TRH may interact with Asn-110 in TM-3 and with Asn-289 in ECL-3; N110A and N289A TRH-Rs exhibit similar apparent affinities that are only 20−30-fold lower than wild-type TRH-R. To better understand these findings, we analyzed a computer-generated model which predicts that the ECLs form an entry channel into the TRH-R TM bundle, that Tyr-181 projects into this channel and that the pyroGlu of TRH cannot simultaneously interact with residues in the TMs and ECLs. Kinetic analysis showed that the association rate of [N^{τ}-*methyl*-His]TRH with N289A TRH-R is slower than with wild-type TRH-R and largely accounts for the lower apparent affinity; the association rate with N110A TRH-R is similar to that of wild-type TRH-R. These data are consistent with the idea that there are initial interactions between TRH and the residues of a putative entry channel of TRH-R. We suggest that a role of the ECLs in all G protein-coupled receptors for small ligands may be to initially contact the ligand and allow entry into a TM binding pocket.

The thyrotropin-releasing hormone (TRH)[1] receptor (TRH-R) belongs to the rhodopsin/β-adrenergic receptor subfamily of seven transmembrane-spanning, G protein-coupled receptors (GPCRs) (*1*). We have recently proposed a model of the TRH-R that places the binding pocket for TRH within the receptor transmembrane helical (TM) bundle (*2*). This prediction is consistent with findings for the position of the binding pockets for small ligands in other GPCRs (*3*). The model is based on evidence in support of four direct contacts between TRH (pyroglutamic acid-histidine-prolinamide; pyroGlu-His-ProNH_2) and TRH-R: Tyr at position 106 (Tyr-106) and Asn-110 in TM-3 with the ring of pyroGlu; Tyr-282 in TM-6 with His; and Arg-306 in TM-7 with the terminal carboxamide of ProNH_2 (*2*, *4*). These interactions were established through the use of complementary substitutions of residues in TRH and TRH-R and the loss of ability of mutant receptors to recognize differences between TRH and its analogues. In the case of Asn-110, a mutant TRH-R in which Asn-110 was substituted by Ala (N110A TRH-R) was found to have an approximately 30-fold lowered affinity for [N^{τ}-*methyl*-His]TRH (MeTRH) compared to WT TRH-R and a decreased ability to differentiate between TRH and an analogue in which the ring N-H of the pyroglutamyl (pyroGlu) moiety of TRH was substituted by O (*5*). These findings are consistent with an interaction between Asn-110 and the pyroGlu moiety of TRH. Other investigators have presented evidence that Asn-289 in extracellular loop 3 (ECL-3) interacts with the pyroGlu moiety also (*6*).

For large ligands such as glycoprotein hormones, the high-affinity binding interactions are with residues in the extracellular domains; for small ligands, such as biogenic amine neurotransmitters, the high-affinity binding pocket is within the TM domains; and for moderate-sized peptides, such as angiotensin, there is evidence that both extracellular and TM domains contribute to the binding pocket (see refs *7*−*9* for reviews). Han and Tashjian have shown that the amino terminus and ECL-1 of TRH-R do not directly contact TRH and that ECL-2 and ECL-3 are important for high-affinity binding (*6*, *10*). We find evidence in support of interactions of TRH with residues in ECL-2 and ECL-3. Through computational and kinetic analyses, we provide evidence that

† This work was supported by National Institutes of Health Physician Scientist Award DK 02101 (to J.H.P.), National Research Service Award DK 09647 (to A.-O.C.), and Grant DK 43036 (to M.C.G. and R.O.).

* To whom correspondence should be addressed: Cornell University Medical College, 1300 York Ave., Room A328, New York, NY 10021. Telephone 212 746-6280; Fax 212 746−6289; E-mail jhperlma@mail.med.cornell.edu.

‡ Cornell University Medical College and The New York Hospital.

§ Mount Sinai School of Medicine and the City University of New York.

|| NIDDK, NIH.

⊥ Deceased.

⊗ Abstract published in *Advance ACS Abstracts,* December 1, 1997.

[1] Abbreviations: TRH, thyrotropin-releasing hormone; TRH-R, thyrotropin-releasing hormone receptor; GPCR, G protein-coupled receptor; TM, transmembrane; pyroGlu, pyroglutamyl; ECL, extracellular loop; MeTRH, [N^{τ}-methyl-His]TRH; k_{on}, association rate constant; IPs, inositol phosphate second messengers.

S0006-2960(97)01331-7 CCC: $14.00

the role of the ECLs is to form a channel that initially binds TRH and allows for entry of TRH into a TM binding pocket.

MATERIALS AND METHODS

Materials. [^{3}H]MeTRH was obtained from DuPont. *myo*-[^{3}H]inositol was obtained from Amersham. TRH was from Calbiochem and MeTRH from Sigma. [DesazapyroGlu]-TRH (desaza^{1}TRH, (N^{α}-[(1*R*)-(3-oxocyclopentyl)carbonyl]-L-histidyl-L-prolineamide) was synthesized by a modification of a previously published procedure (*11*). Val^{2}TRH was from Peninsula and Pyr^{3}TRH was a gift from Dr. T. K. Sawyer (Parke-Davis Pharmaceutical Research). Restriction endonucleases were from New England Biolabs. The cloning vector pBluescript was from Stratagene and the expression vector pCDM8 was from Invitrogen. Dulbecco's modified Eagle's medium and Nu-Serum were from Life Technologies.

Mutagenesis. The full-length, mouse TRH-R cDNA in pBluescript (pBSmTRHR) and pCDM8 (pCDM8mTRHR) (*12, 13*) and construction of N110A, C98A, and C179A TRH-Rs were previously described (*5, 14*). The polymerase chain reaction was used to generate fragments containing the Y181F, N289A, F296A, or E298A mutations, which were subcloned into pBSmTRHR. A fragment derived from digestion with *Xho*I and *Not*I was then subcloned into pCDM8mTRHR. Mutations were confirmed by the dideoxy chain-termination method.

Cell Culture and Transfection. COS-1 cells were maintained and transfected as described (*15, 16*). After transfection, cells were maintained in Dulbecco's modified Eagle's medium with 10% Nu-Serum for 1 day, at which time cells were harvested and seeded into 12-well plates at 100 000 cells/well in Dulbecco's modified Eagle's medium with 5% Nu-Serum.

Receptor Binding Studies. Binding experiments were conducted 1 day after reseeding into 12-well plates. Competition binding assays at equilibrium to measure apparent affinity constants were performed at 23 or 37 °C with [^{3}H]MeTRH, which is an analogue of TRH with 5−10-fold higher affinity (*17*), and various concentrations of unlabeled TRH analogues as described (*15*) for 1 or 3 h (N289A TRH-R). Equilibrium binding constants were derived from competition binding experiments using the formula $K_i = (IC_{50})/(1 + ([L]/K_d))$, where IC_{50} is the concentration of unlabeled analogue that half-displaces specifically bound [^{3}H]MeTRH and K_d is the equilibrium dissociation constant of WT TRH-R for [^{3}H]MeTRH. Curves were fitted by nonlinear regression analysis and drawn with the PRISM program (GraphPad Inc.).

Association binding experiments were performed at 23 °C with several concentrations of [^{3}H]MeTRH and specific binding was determined at various time points. The association rate constant (k_{on}) of each TRH-R for [^{3}H]MeTRH was determined by measuring the observed rate constants (k_{obs}) as a function of the concentration of [^{3}H]MeTRH. In the case where [L] >> [R], the reaction is pseudo-first-order and the slope of a plot of the observed rate constant as a function of concentration of radiolabeled ligand [L] is the association rate constant (k_{on}) (*18*).

Inositol Phosphate Formation. One day after transfection, cells in monolayer in 12-well plates were labeled with 1 μCi of *myo*-[^{3}H]inositol/mL. Stimulation of IP formation was measured 1 day later for 1 h at 37 °C by methods previously described (*15*). With receptor−ligand combinations that yield similar maximal responses, relative potencies reflect relative affinities; we have previously demonstrated this for TRH-Rs (*4*).

Modeling of Extracellular Loops. The ECLs were added to a previously constructed model of the TM domain of TRH-R (*2*). The disulfide bridge between Cys residues in ECL-1 and ECL-2, which has been shown to be necessary to maintain a high-affinity form of the TRH-R (*14*), was included throughout all simulations. The model with frozen helices was energy minimized with the program CHARMM (19) and used to generate fourteen energy-minimized average structures through a simulated annealing protocol (*20*). The details of these simulations have been presented elsewhere (*21*). Briefly, the minimized structure was heated to 1500 K and 14 initial structures were extracted from a trajectory at this temperature. Each of these structures was annealed to 300 K over 60 ps followed by 100 ps of constant-temperature simulation at 300 K. The resulting minimized average structures clustered according to their pairwise root-mean square deviation (rmsd), producing a major family of seven members at rmsd of 1.9 Å. One of these structures was used to conduct a simulation of the receptor−TRH complex to monitor the distances to Asn-110, Tyr-181, and Asn-289. TRH was manually placed in the binding pocket determined in a previous work (*2*). All constraints were removed, and the complex was energy-minimized, heated to 300 K in 23 ps, and subjected to 1 ns of molecular dynamics simulation at 300 K. Distances between the Oδ of Asn-110 and the H−N of pyroGlu, between the Oδ of Asn-289 and the H−N of pyroGlu, and between the Oζ of Tyr-181 and N of pyroGlu were monitored throughout the trajectory.

A 1 ns simulation was performed on the unoccupied WT receptor in which the helices were frozen. To examine the effects of mutation of Tyr-181 on receptor structure, a model of the mutant TRH-R was constructed by substituting Phe for Tyr at the end of the 1 ns simulation of the unoccupied WT receptor. The system was energy-minimized and heated to 300 K in 23 ps, and a molecular dynamics simulation was performed at 300 K for 1 ns on the ECLs of the receptor. In all calculations, a distance-dependent dielectric function was used to approximate the effect of the environment.

RESULTS AND DISCUSSION

To begin our investigation of the role of the ECLs, we substituted for residues of ECL-2 and ECL-3 and tested for effects of these substitutions on binding in transiently transfected COS-1 cells. In agreement with prior results (*10*), substitution of Tyr-181 in ECL-2 by Phe resulted in no specific binding of [^{3}H]MeTRH at concentrations up to 10 nM. Substitution of Phe-296 in ECL-3 by Ala did not affect binding compared to WT TRH-R (Table 1). Substitution of Glu-298 in ECL-3 by Ala resulted in a 3-fold loss in apparent affinity; others have reported that E298A TRH-R exhibits the same affinity as WT TRH-R (*10*). To test for interactions between pyroGlu of TRH and ECL residues, we used a TRH analogue, desaza^{1}TRH, in which the N−H of the pyroGlu moiety was substituted by a methylene group, thereby removing a potential hydrogen-bond donor. The apparent affinity of WT TRH-R for desaza^{1}TRH was 130-

Table 1: Binding Affinities of WT and Mutant TRH-Rs for TRH and Desaza[1]TRH at 37 °C[a]

	K_i (μM)		
TRH-R	TRH	desaza[1]TRH	ratio[b]
WT	0.019 (0.017−0.021) ($n = 15$)	2.4 (2.1−2.6) ($n = 11$)	130 (100−150)
Y181F	nsb		
C98A	nsb		
C179A	nsb		
F296A	0.022 (0.019−0.027) ($n = 2$)	1.8 (1.5−2.2) ($n = 2$)	82 (60−120)
E298A	0.059 (0.048−0.073) ($n = 2$)	4.0 (3.2−5.0) ($n = 2$)	68 (40−100)

[a] The data are presented as the mean (95% confidence interval). *n*, number of experiments. The B_{max} / well values for WT, F296A, and E298A TRH-Rs (mean ± SE) were 71 000 ± 2600, 74 000 ± 1700, and 160 000 ± 3500 dpm, respectively, in one experiment and 41 000 ± 1100, 40 000 ± 570, and 110 000 ± 1500 dpm, respectively, in another experiment. [b] Ratio = K_i(desaza[1]TRH)/K_i(TRH). [c] nsb, no specific binding was detectable.

fold lower than for TRH. Compared to TRH, the apparent affinities of F296A and E298A TRH-Rs for desaza[1]TRH were lowered by 82- and 68-fold, respectively, which are not different from the value for WT TRH-R. Because the binding affinities for desaza[1]TRH compared to TRH were lowered to similar extents in F296A and E298A TRH-Rs as in WT TRH-R, we concluded that the pyroGlu moiety of TRH does not directly contact Phe-296 or Glu-298 in the occupied WT TRH-R.

To further investigate the loss of specific binding observed with Y181F TRH-R, stimulation of IP formation was measured (Table 2). In general, estimates of potency reflect affinities in receptors of equal efficacy (*18*). The maximal levels of TRH-stimulated IP formation were similar in cells expressing WT and Y181F TRH-Rs, which is consistent with their efficacies being similar. We have shown that potency does reflect affinity in those mutant TRH-Rs in which efficacy was similar to WT TRH-R and binding could be measured directly (*4*). The EC_{50} of TRH for Y181F TRH-R was 3700-fold higher than that for WT TRH-R. Thus, the lack of specific binding in cells expressing Y181F TRH-Rs was attributable to a loss of affinity and not to a lack of cell-surface expression. These data indicate that Tyr-181 is important for binding. The EC_{50} of desaza[1]TRH for WT TRH-R was 90-fold higher than that of TRH (Table 2), which is not different from the ratio of binding affinities (Table 1). The EC_{50} of desaza[1]TRH for Y181F TRH-R was *lower* than that of TRH; that is, Y181F TRH-R appeared to prefer desaza[1]TRH over TRH. Thus, substitution of Tyr-181 by Phe abolished the ability of TRH-R to select TRH over an analogue in which the ring N−H of pyroGlu was removed. This is consistent with the idea that Tyr-181 contacts the pyroGlu moiety of TRH. To establish the specificity of this selectivity change, we compared the potencies for TRH and desaza[1]TRH of two ECL mutant TRH-Rs that had previously been shown to be of much lower affinity than WT TRH-R. Cys-98 and Cys-179 are highly conserved residues that form a disulfide bond critical for maintaining high-affinity binding of TRH-R that is thought to be critical for maintaining the structure of GPCRs (*14*). C98A and C179A TRH-Rs exhibit no specific [^{3}H]MeTRH binding. The EC_{50}s of C98A and C179A TRH-Rs for TRH were 2200- and 460-fold lower, respectively, than that of WT TRH-R, in agreement with prior findings (*14*). The potencies of C98A and C179A TRH-Rs for desaza[1]TRH were 250- and 180-fold lower than for TRH, which are not different from the relative potencies of TRH and desaza[1]TRH at WT TRH-R. Thus, unlike Y181F TRH-R, there was no loss of ability of C98A or C179A TRH-Rs to distinguish between TRH and desaza[1]TRH. We, therefore, conclude that the loss of ability of Y181F TRH-R to distinguish between TRH and desaza[1]TRH is consistent with a direct interaction between the pyroGlu moiety of TRH and Tyr-181 in ECL-2 of TRH-R. To further confirm the specificity of the selectivity change, the apparent affinities of WT and Y181F TRH-Rs for TRH and analogues substituted at His or prolinamide were compared. We have previously shown that the affinities of WT TRH-R for Val[2]TRH and Pyr[3]TRH (in which the $ProNH_2$ is replaced by pyrrolidine, resulting in substitution of the terminal carboxamide of TRH by H) are lowered by 500- and 640-fold, respectively (*4*). Compared to TRH, the EC_{50}s for activation of WT TRH-R by Val[2]TRH and Pyr[3]TRH are 910- and 940-fold higher. Similarly, compared to TRH, the EC_{50}s for activation of Y181F TRH-R by Val[2]TRH and Pyr[3]TRH are 820- and 840-fold higher. Thus, Y181F TRH-R fully retains the ability to select TRH over analogues substituted at His and $ProNH_2$, in contrast to the complete loss of ability to select TRH over an analogue substituted at pyroGlu.

The experimental data show an apparent interaction between the pyroGlu moiety of TRH and Tyr-181, which is on the surface of the receptor. Since previous work demonstrated that pyroGlu interacts with Tyr-106 and Asn-110 in TM-3, these results suggest that there are at least two binding sites for TRH in TRH-R. One is on the surface of the receptor, as demonstrated by the present results, and the other is in the TM domain, as demonstrated by our previous work. Our model of the TM binding pocket of TRH-R is consistent with interactions of pyroGlu with Asn-110 and Tyr-106 (*2*, *4*). To better understand the present results, we developed a model of TRH-R that includes the ECLs. Starting from the structure predicted by our previous simulations (*2*), we conducted extended (1 ns) molecular dynamics simulations on the complex between the new WT TRH-R model and TRH as described in Experimental Procedures. To explore the role in binding for the ECLs, we conducted a 1 ns simulation of the ECLs of the unoccupied WT TRH-R. The arrangement of the ECLs in WT TRH-R generates a cavity that can serve as a putative surface binding site (*21*). This cavity includes Tyr-181, Asn-289, Phe-296, and Glu-298 (Figure 1). Its bottom is formed by Lys-182, and movement of this residue exposes the TM binding pocket. This structure is consistent with the idea that TRH initially interacts with the binding site on the surface of the receptor and then moves into the TM binding pocket by inducing a conformational change that "opens" an entry channel.

Our model shows that the distance between Tyr-106 in the TM binding site and Tyr-181 on the surface is 17 Å (Figure 1). Likewise, the distance between Asn-110 and Asn-289 in ECL-3 is 20 Å. Such distances would preclude a simultaneous interaction of pyroGlu with the residues in the TM binding site and the residues on the receptor surface. To gain further insight into the spatial relation of TRH to the putative TM and ECL binding sites, we monitored the

Table 2: Activation Potencies of WT and Mutant TRH-Rs for TRH Analogues[a]

	(EC_{50} (μM)						
TRH-R	TRH	desaza[1]TRH	ratio[b]	Val[2]TRH	ratio[c]	Pyr[3]TRH	ratio[d]
WT	0.00068 (0.00054−0.00085) ($n = 7$)	0.061 (0.045−0.082) ($n = 6$)	90 (53−150)	0.62 (0.45−0.83) ($n = 2$)	910 (660−1700)	0.64 (0.5−0.81) ($n = 4$)	940 (590−1500)
Y181F	2.5 (2.1−3.0) ($n = 3$)	0.75 (0.55−1.0) ($n = 3$)	0.34 (0.2−0.5)	2300 (2100−2600) ($n = 2$)	820 (700−1200)	2100 (1900−2400) ($n = 2$)	840 (600−1100)
C98A	1.5 (1.2−1.8) ($n = 2$)	380 (340−420) ($n = 2$)	250	nd[e]		nd	
C179A	0.31 (0.22−0.43) ($n = 2$)	55 (45−68) ($n = 2$)	180	nd		nd	

[a] The data are presented as the mean (95% confidence interval). *n*, number of experiments. [b] Ratio = EC_{50}(desaza[1]TRH)/EC_{50}(TRH). [c] Ratio = EC_{50}(Val[2]TRH)/EC_{50}(TRH). [d] Ratio = EC_{50}(Pyr[3]TRH)/EC_{50}(TRH). [e] nd, not determined.

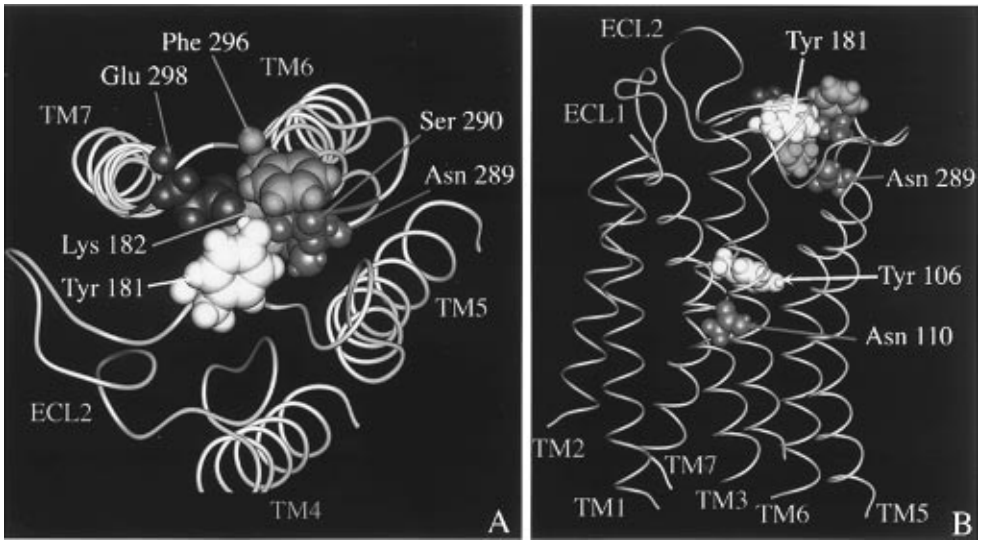

FIGURE 1: Space-filling representation of selected residues that define the putative surface binding site viewed from the extracellular domain (A) and in side view (B).

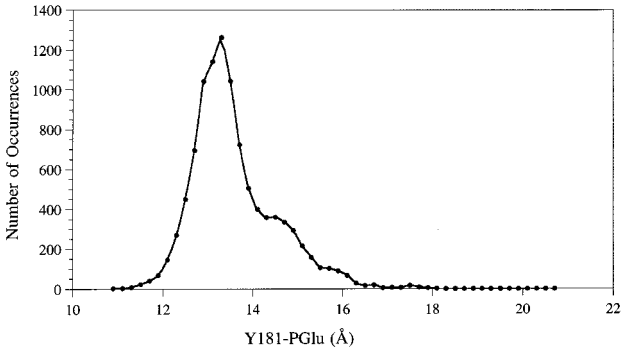

FIGURE 2: Distribution of the distance between the nitrogen of pyroGlu (PGlu) of TRH and the Oζ of Tyr-181 (Y181) during a 1 ns molecular dynamics simulation of TRH-R with TRH in the TM binding pocket. Each point represents the number of times a distance within 0.2 Å is observed during the simulation. The sum of all occurrences is 10 000, which is the number of structures recorded during the simulation.

distance between pyroGlu and Tyr-181 during the course of the simulation of TRH-R with TRH in the TM binding pocket. Our results show that the distance from pGlu to Oζ of Tyr-181 averages 13.5 Å and is never less than 11 Å (Figure 2). This indicates that pyroGlu cannot interact with residues in the TM and the ECL domains simultaneously.

The substitution of Tyr-181 by Phe results in a significant change in the affinity of TRH to the receptor. Part of the nearly 4000-fold reduction in affinity can be attributed to the elimination of the Tyr hydroxyl group, which could be responsible for a H-bonding interaction with the pyroGlu moiety. This is corroborated by the reduced ability of Y181F TRH-R to discriminate between TRH and desaza[1]TRH. We also note that the H-bonding network previously observed in the putative surface binding pocket (*21*) is significantly affected by the mutation. Previous work showed that, in the unoccupied WT TRH-R, Lys-182 lines the bottom of the surface binding site by forming H-bonds with the side chains of Ser-290 and Glu-298, which is itself H-bonded to the OH group of Tyr-181. To analyze the changes, we have monitored these three H-bonds by determining their sampling distribution probabilities in a 1 ns trajectory (Figure 3A). In WT TRH-R, the Y181−E298 and K182−E298 H-bonds have narrow distributions with average values of 2.49 and 2.65 Å, respectively, while the distribution of the H-bond between Lys-182 and Ser-290 is wider, with an average value of 2.90 Å. To quantitate the fraction of H-bonds maintained during the 1 ns simulation, we used the average H-bond distances to which one standard deviation was added as cutoff values. As shown in Figure 4A, the Y181−E298 H-bond is maintained at a value of 2.55 Å 82% of the time, the K182−E298 H-bond is maintained at 2.75 Å 87% of the time and the K182−S290 H-bond is maintained at 3.10 Å

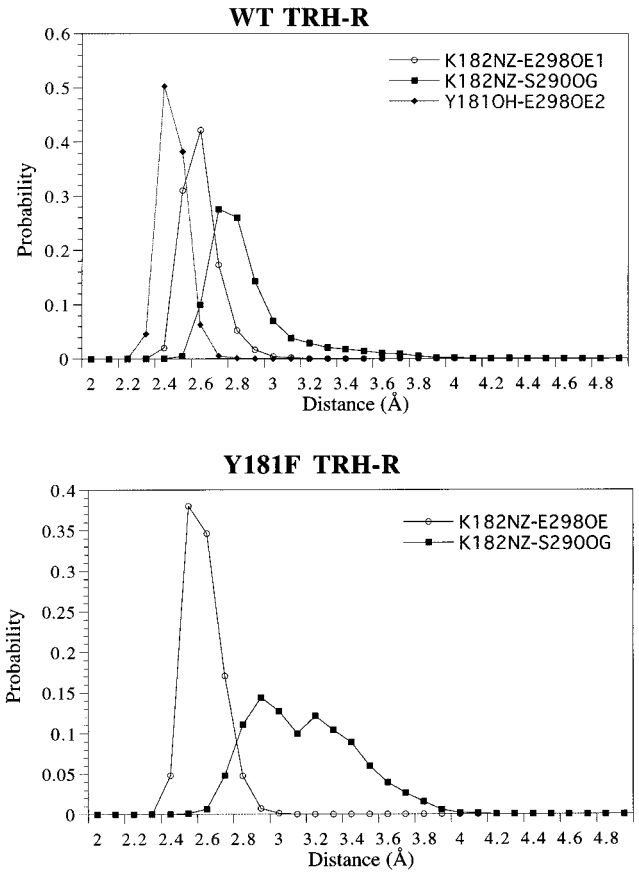

FIGURE 3: (Top) Sampling distribution probabilities of H-bonds between Lys-182 (K182), Glu-298 (E298), and Ser-290 (S290) in a 1 ns simulation of the unoccupied WT TRH-R. Each point represents the probability of finding the system in a displacement interval of 0.1 Å as a function of distance. (Bottom) Sampling distribution probabilities of H-bonds between Lys-182 (K182), Glu-298 (E298), and Ser-290 (S290) in a 1 ns simulation of the unoccupied Y181F TRH-R. The H-bond between Lys-182 and Glu-298 represents the shortest of the K182NZ−E298OE1 or K182NZ−E298OE2 distances.

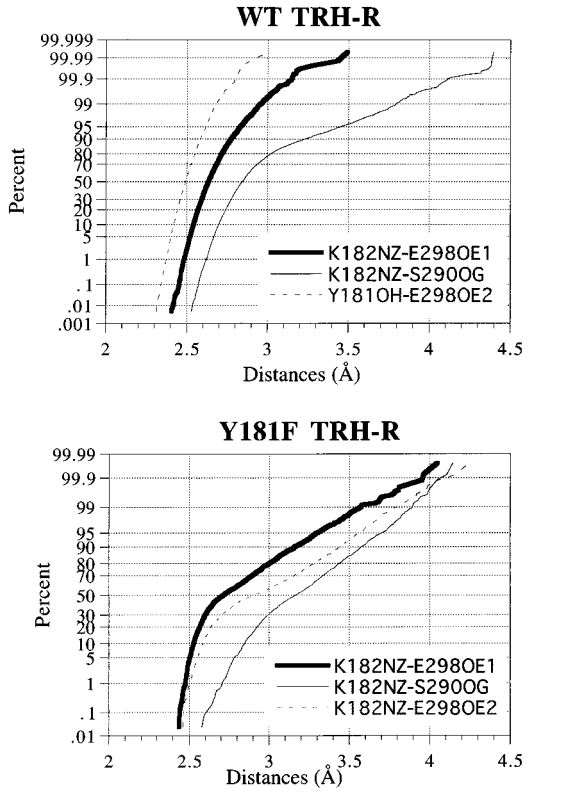

FIGURE 4: Cumulative percentage probability of distances between Lys-182 (K182), Glu-298 (E298), and Ser-290 (S290) in the unoccupied WT and Y181F TRH-Rs.

85% of the time. Such behavior is characteristic of undisrupted H-bonds. In the Y181F mutant receptor, elimination of the OH group of Tyr-181 leads to further changes in the distribution of the distances between Lys-182 and both Ser-290 and Glu-298. The major change is in the distance between the side chains of Lys-182 and Ser-290. This distance oscillates between 2.6 and 4.0 Å during a 1 ns simulation (Figure 3B) and remains at the 3.1 Å cutoff distance determined in the WT TRH-R only 43% of the time (Figure 4B). The distance between Lys-182 and Glu-298 shows a time-dependent change. During approximately 500 ps of simulation, the H-bond to one of the Oϵ of Glu-298 is maintained and then Lys-182 turns to form a stable H-bond with the other Oϵ. In this simulation, Lys-182 is H-bonded to Glu-298 at the cutoff value of 2.75 Å 88% of the time, but fluctuates between the two oxygens of Glu-298. In the WT TRH-R, however, only one Oϵ of Glu-298 interacted with Lys-182, while the other one formed a hydrogen bond to Tyr-181. These results show a disorganized putative surface binding pocket in the mutant receptor that may partially contribute to the estimated 3700-fold affinity loss for TRH upon removal of the phenolic group of Tyr-181.

The disruption of the H-bonding network leads also to changes in mobility of the surface binding pocket that could further contribute to loss in affinity. We examined the mobility of Tyr-181, Lys-182, Asn-289, Phe-296, and Glu-298 by calculating the ratios in the variance of atomic displacements around the average of the last 500 ps in the simulation of WT TRH-R and that of the Y181F mutant receptor. The logarithm of this ratio is directly proportional to the difference in the vibrational entropies of the two receptors. Figure 5 shows large ratios indicative of changes in mobility for atoms in the residue at position 181, Lys-182, and Glu-298 upon mutating Tyr-181 to Phe. Examination of the changes in mobility of these residues as well as other residues of the loops (*e.g.*, Tyr-95, Phe-291) indicate that the vibrational entropy of the loops in the mutant receptor is higher than in WT TRH-R. Thus, if the interaction with the ligand freezes certain motions of the loops, the increased mobility of the mutant receptor will contribute to the lower apparent affinity through an entropic effect. It, therefore, appears that mutation of Tyr-181 to Phe results in a loss of a H-bonding group and a less organized surface binding pocket. The resulting increased mobility of residues in the ECLs may lead to decreased binding capabilities of the ligand to the surface of its receptor by increasing its entropy.

Upon investigating the conformational properties of Tyr-181 in our model, we observed that Asn-289 was among several residues positioned between the surface binding site and the TM binding pocket. According to the proposed sequential binding process, Asn-289 would interact with TRH in the course of its movement from the surface to the TM binding site. Previous work suggested that Asn-289 could interact with TRH (*6*). We have confirmed this finding by performing binding experiments on the N289A mutant receptor (Table 3), and our results show a 20-fold decrease in the apparent affinity of N289A TRH-R compared to WT TRH-R. This decrease in affinity is approximately the same as that observed upon mutating Asn-110 to Ala, a residue

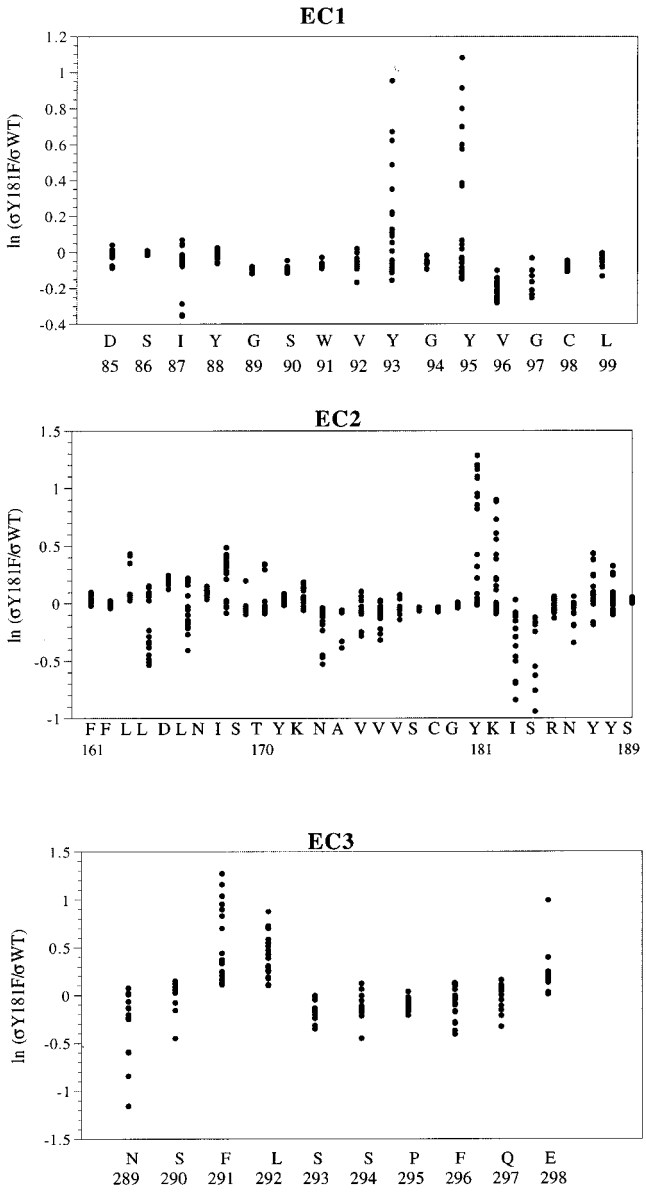

FIGURE 5: Logarithm of the ratios of the variance of atomic displacements around the average in the last 500 ps in the simulations of the unoccupied Y181F TRH-R versus that of the unoccupied WT TRH-R. Each atom is represented by a point. A positive ratio means that Y181F TRH-R is more mobile than WT TRH-R. A negative ratio means that WT TRH-R is more mobile than Y181F TRH-R.

Table 3: Affinities and Rate Constants for WT, N289A, and N110A TRH-Rs at 23 °C

	WT	N289A	N110A
K_d (nM)	1.1[b]	22 (17−28) ($n = 3$)	33 (27−41) ($n = 3$)
k_{on} (μM^{-1} min^{-1})	21 (15−27) ($n = 11$)	2.7 (0−7) ($n = 5$)	56 (20−93) ($n = 6$)

that we have previously shown to interact with the pyroGlu moiety of TRH (*5*). Since Asn-289 is positioned at the beginning of ECL-3 and, contrary to Tyr-181, is not fully exposed at the surface of the receptor, we have measured the distances between pyroGlu of TRH and both Asn-110 and Asn-289 to gain further understanding into the binding of TRH to these two residues. The distances between the pyroGlu of TRH and Asn-110 in the course of the 1 ns simulation were inversely related to those between pyroGlu and Asn-289, and two distinct populations of structures were observed (Figure 6). Thus, although the binding data suggest that the pyroGlu of TRH may interact with both Asn-110 and Asn-289, computer simulations predict that pyroGlu of TRH cannot be close to Asn-110 and Asn-289 simultaneously. This analysis supports the suggestion that pyroGlu of TRH first interacts with Asn-289 in the entry channel and then with Asn-110 in the TM pocket.

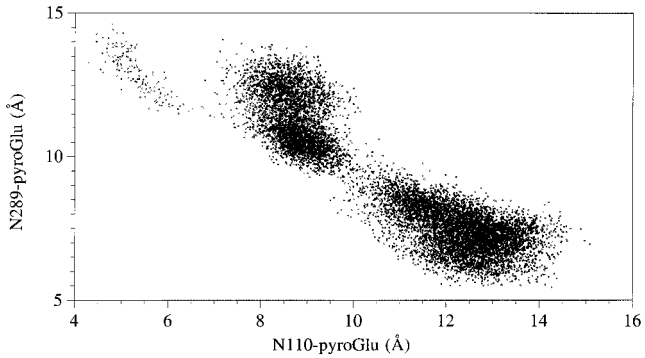

FIGURE 6: Distribution of the distances between Asn-110 (N110) and Asn-289 (N289) of TRH-R and the N−H group of pyroGlu of TRH during a 1 ns molecular dynamics simulation of the complex with TRH in the TM binding pocket of WT TRH-R. The distances between the Oδ of Asn-110 and of Asn-289 and the H−N of pyroGlu were monitored throughout the simulation.

If Asn-289 is indeed positioned in the entry channel, we hypothesized that mutation to Ala should result in the elimination of an initial anchoring site for TRH and hence should affect the association kinetics. On the other hand, since Asn-110 is deeply buried in the TM domain, the rate of association of TRH should not depend on the mutation N110A. To test this hypothesis, we measured the time dependence of binding of [^{3}H]MeTRH to WT, N110A, and N289A TRH-Rs. The MeTRH association rate constant (k_{on}) for N110A TRH-R was not different from that for WT TRH-R, whereas that for N289A TRH-R was 8-fold slower than for WT TRH-R (Table 3). Thus, Asn-289 contributes to association of MeTRH with TRH-R and the decrease in the rate of ligand association is a major contributing factor to the 20-fold decrease in affinity of N289A TRH-R compared to WT TRH-R. In contrast, Asn-110 does not appear to contribute to association and the 30-fold decrease in affinity of N110A TRH-R must be due to an increase in the rate of its dissociation. [Our attempts to analyze dissociation experiments have been hampered by the multicomponent nature of dissociation from TRH-Rs (*22*). We are attempting to develop a quantitative method for this analysis.] These data are consistent with the idea that TRH binds first to the ECLs and then to the TM bundle of TRH-R.

Our data indicate that substitution of Tyr-181 in ECL-2 by Phe can change the ability of TRH-R to recognize a TRH analogue missing the ring N-H of the pyroGlu moiety. Removal of the phenolic group at position 181 resulted in an apparent 3700-fold affinity loss for TRH. Importantly, selectivity in favor of TRH versus desaza[1]TRH was completely abolished; there may even be a small preference for desaza[1]TRH over TRH. These data are consistent with a critical role for Tyr-181 in the recognition of the pyroGlu of TRH. The possible preference of Y181F TRH-R for desaza[1]TRH may be due to an interaction between the ring methylene group that has been introduced in pyroGlu and

the nonpolar aromatic group of the Phe introduced at position 181 of Y181F TRH-R.

Our experimental and modeling data are most consistent with the idea that TRH interacts directly with the extracellular loops although other possibilities have not been completely excluded. For example, it is possible that a substitution in the ECLs could alter the conformation of TRH-R in such a way as to indirectly affect the TM binding pocket for TRH. We consider such an allosteric model to be less likely than the model we propose, since it does not as easily explain the loss of selectivity and decreased association kinetics resulting from substitution of ECL residues. Indirect approaches such as ours must be used to assess direct contacts between ligand and receptor until biophysical methods are available to analyze GPCR interactions. The use of additivity of effects to assess direct interactions has been previously reviewed and supported (*23*−*25*).

Our data are consistent with two states of interaction involving TRH-R and the pyroGlu moiety of TRH. We previously showed that TM-3 contacts the pyroGlu of TRH (*26*). Y106F TRH-R exhibits an apparent 100 000-fold affinity decrease for TRH and an almost complete loss of selectivity for a TRH analogue in which pyroGlu has been substituted. Both N110A TRH-R and N289A TRH-R exhibited a lowered affinity for TRH compared to WT TRH-R and a decreased ability to discriminate between TRH and analogues altered at pyroGlu. Our model indicates that these two TRH-R domains cannot simultaneously bind the pyroGlu of TRH. An entry channel in the ECLs including Tyr-181 and Asn-289 is consistent with the idea that pyroGlu first interacts with an ECL site. This interaction is followed by entry of TRH into the TM domain. In fact, the initial interaction at the surface of TRH-R may serve to position TRH for access into the TM binding pocket. In the TM bundle, the pyroGlu of TRH contacts TM-3 and, in addition, the His and ProNH_2 of TRH contact Tyr-282 in TM-6 and Arg-306 in TM-7, respectively (*26*). The model predicts that movement of Lys-182, located in the floor of the entry channel, allows for movement of TRH into the TM binding pocket. Our experimental analyses indicate that TRH binds initially to ECL residues and then to TM residues. Our model predicts that these ECL residues form part of a putative entry channel. The next step will be to provide further experimental evidence in support of an entry channel.

To our knowledge, a multistep mechanism for binding of small ligands to GPCRs has not been described previously. It has been suggested that large ligands, such as glycoprotein hormones (*27*, *28*) and polypeptides (*29*, *30*), may interact primarily with the extracellular amino termini of GPCRs and that these interactions are followed by secondary interactions with the remainder of receptor. It has been proposed that TM residues near the extracellular surface may filter access of ligands to the TM bundle (*31*). These proposals, however, have not been supported by kinetic or computational analyses.

In conclusion, our findings are consistent with the idea that the pyroGlu of TRH binds to at least two discrete domains of TRH-R. Our model and kinetic analyses suggest that TRH interacts initially with residues in an entry channel formed by the ECLs and then moves into the TM binding pocket. We suggest that sequential binding interactions similar to these between TRH and TRH-R may occur between other small ligands and their GPCRs and that small ligands may be guided into TM binding pockets by ECLs.

REFERENCES

1. Strader, C. D., Fong, T. M., Tota, M. R., Underwood, D., and Dixon, R. A. F. (1994) *Annu. Rev. Biochem. 63*, 101−132.
2. Laakkonen, L., Guarnieri, F., Perlman, J. H., Gershengorn, M. C., and Osman, R. (1996) *Biochemistry 35*, 7651−7663.
3. Van Rhee, A. M., and Jacobson, K. A. (1996) *Drug Dev. Res. 37*, 1−38.
4. Perlman, J. H., Laakkonen, L. J., Guarnieri, F., Osman, R., and Gershengorn, M. C. (1996) *Biochemistry 35*, 7643−7650.
5. Perlman, J. H., Laakkonen, L., Osman, R., and Gershengorn, M. C. (1994) *J. Biol. Chem. 269*, 23383−23386.
6. Han, B. M., and Tashjian, A. H., Jr. (1995) *Biochemistry 34*, 13412−13422.
7. Baldwin, J. M. (1993) *EMBO J. 12*, 1693−1703.
8. Strader, C. D., Fong, T. M., Graziano, M. P., and Tota, M. R. (1995) *FASEB J. 9*, 745−754.
9. Schwartz, T. W. (1994) *Curr. Opin. Biotechnol. 5*, 434−444.
10. Han, B. M., and Tashjian, A. H., Jr. (1995) *Mol. Endocrinol. 9*, 1708−1719.
11. Uchida, I., Saito, A., Yasuda, A., Iwata, K., Hari, H., Hara, K., Matsushita, M., Anami, K., Haruta, J., and Furukawa, N. (1993) *Chem. Abstr. 119*, 117836.
12. Straub, R. E., Frech, G. C., Joho, R. H., and Gershengorn, M. C. (1990) *Proc. Natl. Acad. Sci. U.S.A. 87*, 9514−9518.
13. Gershengorn, M. C., and Thaw, C. N. (1991) *Endocrinology 128*, 1204−1206.
14. Perlman, J. H., Wang, W., Nussenzveig, D. R., and Gershengorn, M. C. (1995) *J. Biol. Chem. 270*, 24682−24685.
15. Perlman, J. H., Thaw, C. N., Laakkonen, L., Bowers, C. Y., Osman, R., and Gershengorn, M. C. (1994) *J. Biol. Chem. 269*, 1610−1613.
16. Perlman, J. H., Laakkonen, L., Osman, R., and Gershengorn, M. C. (1995) *Mol. Pharmacol. 47*, 480−484.
17. Vale, W., Rivier, J., and Burgus, R. (1971) *Endocrinology 89*, 1485−1488.
18. Limbird, L. E. (1986) *Cell surface receptors: A short course on theory and methods*, Martinus Nijhoff Publishing, Boston, Dordrecht, and Lancaster.
19. Brooks, B. R., Bruccoleri, R. E., Olafson, B. D., States, D. J., Swaminathan, S., and Karplus, M. (1983) *J. Comput. Chem. 4*, 187−217.
20. Kirkpatrick, S., Gelatt, C. D., Jr., and Vecchi, M. P. (1983) *Science 220*, 671−680.
21. Colson, A. O., Perlman, J. H., Smolyar, A., Gershengorn, M. C., and Osman, R. (1997) Static and dynamic roles of extracellular loops in G-protein coupled receptors: A mechanism for sequential binding of thyrotropin-releasing hormone to its receptor, *Biophys. J.* (in press).
22. Hinkle, P. M., and Kinsella, P. A. (1982) *J. Biol. Chem. 257*, 5462−5470.
23. Wells, J. A. (1990) *Biochemistry 29*, 8509−8517.
24. LiCata, V. J., and Ackers, G. K. (1995) *Biochemistry 34*, 3133−3139.
25. Mildvan, A. S., Weber, D. J., and Kuliopulos, A. (1992) *Arch. Biochem. Biophys. 294*, 327−340.
26. Gershengorn, M. C., and Osman, R. (1996) *Physiol. Rev. 76*, 175−191.
27. Xie, Y.-B., Wang, H., and Segaloff, D. L. (1990) *J. Biol. Chem. 265*, 21411−21414.
28. Ji, I., and Ji, T. H. (1991) *J. Biol. Chem. 266*, 13076−13079.
29. Stroop, S. D., Kuestner, R. E., Serwold, T. F., Chen, L., and Moore, E. E. (1995) *Biochemistry 34*, 1050−1057.
30. Monteclaro, F. S., and Charo, I. F. (1996) *J. Biol. Chem. 271*, 19084−19092.
31. Turner, P. R., Bambino, T., and Nissenson, R. A. (1996) *J. Biol. Chem. 271*, 9205−9208.
32. Perlman, J. H., Nussenzveig, D. R., Osman, R., and Gershengorn, M. C. (1992) *J. Biol. Chem. 267*, 24413−24417.

BI9713310